Article

Maternal obesity damages the median eminence blood-brain barrier structure and function in the progeny: The beneficial impact of cross-fostering by lean mothers

Roberta Haddad-Tóvolli[1,2,*], Joseane Morari[1], Roberta Barbizan[1], Vanessa C. Bóbbo[1], Rodrigo S. Carraro[1,3], Carina Solon[1], Nathalia R. Dragano[1], Márcio A. Torsoni[4], Eliana P. Araujo[1,5], Licio A. Velloso[1,*]

[1]Laboratory of Cell Signaling, Obesity and Comorbidities Research Center, State University of Campinas, Brazil

[2]Neuronal Control of Metabolism (NeuCoMe) Laboratory, Institut d'Investigacions Biomèdiques August Pi i Sunyer (IDIBAPS), Barcelona, Spain

[3]Center for Anatomy Studies, University San Francisco (USF), Bragança Paulista, Brazil.

[4]Laboratory of Metabolic Disorders, Faculty of Applied Sciences, UNICAMP, Limeira, Brazil

[5]School of Nursing, University of Campinas, Brazil

***Corresponding authors:** lavellos@unicamp.br; haddad@recerca.clinic.cat

Abstract

Maternal obesity is an important risk factor for obesity, cardiovascular, and metabolic diseases in the offspring. Studies have shown that it leads to hypothalamic inflammation in the progeny, affecting the function of neurons regulating food intake and energy expenditure. In adult mice fed a high-fat diet, one of the hypothalamic abnormalities that contribute to the development of obesity is the damage of the blood-brain barrier (BBB) at the median eminence-arcuate nucleus (ME-ARC) interface; however, how the hypothalamic BBB is affected in the offspring of obese mothers requires further investigation. Here, we used confocal and transmission electron microscopy, transcript expression analysis, glucose tolerance testing, and a cross-fostering intervention to determine the impact of maternal obesity and breastfeeding on BBB integrity at the ME-ARC interface. The offspring of obese mothers were born smaller; conversely, at weaning they presented larger body mass and glucose intolerance. In addition, maternal obesity induced structural and functional damage of the offspring's ME-ARC BBB. By a cross-fostering intervention, some of the defects in barrier integrity and metabolism seen during development in an obesogenic diet were recovered. The offspring of obese dams breastfed by lean dams presented a reduction of body mass and glucose intolerance as compared to the offspring continuously exposed to an obesogenic environment during intrauterine and perinatal life; this was accompanied by partial recovery of the anatomical structure of the ME-ARC interface, and by the normalization of transcript expression of genes coding for hypothalamic neurotransmitters involved in energy balance and BBB integrity. Thus, maternal obesity promotes structural and functional damage of the hypothalamic BBB, which is, in part, reverted by lactation by lean mothers.

Keywords: hypothalamus, blood-brain barrier, maternal programming, obesity, diabetes, breastfeeding

New & Noteworthy

Maternal dietary habits directly influence offspring health. In this study, we aimed at determining the impact of maternal obesity on BBB integrity. We show that DIO offspring presented a leakier ME-BBB, accompanied by changes in the expression of transcripts encoding for endothelial and tanycytic proteins, as well as of hypothalamic neuropeptides. Breastfeeding in lean dams was sufficient to protect the offspring from ME-BBB disruption, providing a preventive strategy of nutritional intervention during early life.

Introduction

The excessive consumption of dietary fats triggers an inflammatory response in the hypothalamus promoting functional and structural damage of neurons involved in the regulation of food intake and energy expenditure (13, 15, 31). In addition to neuronal damage, dietary fats disrupt the proper function of the blood-brain barrier (BBB) in the interface between the median eminence (ME) and the arcuate nucleus (ARC) (2, 22, 36). As in other circumventricular organs, the BBB at the ME is more permissive than in other brain regions, allowing the trafficking of peptides from the hypothalamus to the portal capillary system, as well as the passage of nutrients and blood-born signals from the systemic circulation to the brain (10, 38). This particular property of the ME-BBB is extremely important for hypothalamic function, as it controls, for example, nutrient and hormonal access (including leptin and insulin) to the mediobasal hypothalamus (MBH), where they regulate the function of key neurons involved in the control of whole-body energy balance (2, 19, 24). At least in part, ME-BBB function depends on specialized radial glial cells called tanycytes, which line along the third ventricle wall (16, 32, 44). Tanycytes sense the nutrient status of the organism and dynamicaly adapt to the body's own metabolic state (20, 29, 30). In diet-induced obese (DIO) mice, there is a loss of organization of the ME tanycytes resulting in a leakier barrier and in an exacerbation of hypothalamic inflammation (36). Approaches aimed at preserving the ME-BBB integrity can contribute to mitigate the harmful effects of dietary fats and protect against obesity (27, 36).

Most studies evaluating the impact of dietary fats on hypothalamic integrity were performed in adult rodents. However, it is widely documented that maternal dietary habits, including maternal obesity, affect the development of hypothalamic centers regulating energy homeostasis in the offspring, and significantly increase the probability of developing postnatal metabolic disorders, such as obesity and type 2 diabetes (DM2) (9, 14, 21, 39). In rodents, the melanocortin system begins its organization during embryonic life and completes its maturation postnatally with the assembly of functional neuronal circuitries (12). The specification and maturation of the neurons composing the melanocortin system, mainly pro-opiomelanocortin (POMC) and agouti-related peptide (AgRP), require a complex interplay between molecular, cellular, and nutritional factors acting during a particular developmental window (4). Disruptions in this intricate mechanism during intrauterine and early postnatal life can impair maturation

and function of the system impacting systemic metabolism and energy balance (7, 14). In addition, maternal DIO leads to an abnormal spatial distribution of proopiomelanocortin (POMC) neurons (21) and its axonal projections to target nuclei (21, 34, 42). It also promotes inflammation and disrupts the unfolded protein response in the hypothalamus (9, 34, 37, 41).

Changes in the development of the BBB in the hypothalamus, particularly in the vicinity of the ME, may predispose to obesity (26, 30). Maternal obesity increases BBB permeability in the offspring (26), leading to greater exposure to leptin and ghrelin. Nevertheless, how maternal obesity affects the development of the ME-BBB in the offspring and how nutitional interventions during lactation possibly revert these effects is currently unkown. In this study, we hypothesized that maternal obesity promotes changes in the structure and function of the ME-BBB in the offspring. We show that offspring of obese dams presented a leakier ME-BBB at weaning and was accompanied by changes in the expression of transcripts encoding for endothelial and tanycytic proteins, as well as of hypothalamic neuropeptides. In addition, we show that breastfeeding of DIO offspring by lean dams is sufficient to partially protect the offspring from ME-BBB disruption and metabolic impairments.

Methods

Animal care and diets

Swiss mice were housed under specific pathogen-free conditions, maintained in a temperature-controlled room (22°C) with a 12-h light/dark cycle and free access to food and water. Six-week-old females were separated in two groups according to the type of diet. Control females received Chow diet (Nuvilab) (3.85 kcal/g; 19.2g/100g protein, 67.3g/100g carbohydrate, and 4.3g/100g fat), and high-fat diet females received HFD (5.4 kcal/g; 24g/100g protein, 24g/100g carbohydrate, and 41g/100g fat) over 4 weeks. After this, females were crossed and the offspring were collected at specific stages of development (at birth (P0) and at weaning (P21)). Litter size average was not affected by diet and litters were adjusted (between P1–P4) to six to eight pups to ensure adequate and standardized nutrition until weaning. The experimental procedures involving mice were performed in accordance with the guidelines of the Brazilian College for

Animal Experimentation and were approved by the Ethics Committee of the University of Campinas (CEUA number 3934-1).

Perinatal cross-fostering

To analyze the specific effects of lactation on neuronal programming and BBB structure and function, the offspring of chow-fed dams (Chow-O) and high-fat diet dams (HFD-O) were cross-fostered at the day of birth to females kept on different diets from the offspring until weaning. As a result, a litter originating from a chow dam was allocated to a HFD dam, whereas the litter from the HFD dam was allocated to the chow dam. To control the cross-fostering strategy per se, chow and HFD offspring were cross-fostered to a different chow and HFD dam, respectively. Thus, the cross-fostering strategy resulted in four different groups: (1) chow-offspring kept in chow during lactation (COCL); (2) chow-offspring cross-fostered by HFD dams during lactation (COHL); (3) HFD-offspring cross-fostered by chow dams during lactation (HOCL); (4) HFD-offspring kept under HFD during lactation (HOHL). Litter size was adjusted to six to eight pups as described previously.

Physiological measurements

Maternal and offspring body weight measurements were performed weekly. For the glucose tolerance tests, mice were acutely treated with a single intraperitoneal injection of glucose 25% (2.0 mg/kg) after 6 hours fasting and blood glucose levels were measured at baseline and at 15, 30, 60, 90, and 120 minutes after glucose administration.

Quantitative expression analysis

Medio-basal hypothalami of P0 and P21 mouse offspring were carefully dissected and rapidly frozen in liquid nitrogen. Total RNA extraction was performed by RNeasy Micro Kit (Cat No. 74004, Qiagen) according to manufacturer's instructions. cDNA was generated by PCR reverse transcription using High Capacity cDNA Reverse Transcription Kit (Life Technologies).

PCR Array

A Mouse Tight Junctions PCR Array RT^2 Profiler (PAMM-143Z, Qiagen, USA) consisting of 84 target genes was used in order to seek for candidate genes that could be modulated by HFD during intrauterine development and lactation. 30ng of cDNA, 5.0 µl of QuantiFast SYBR Green PCR Kit (Cat No. 204056, Qiagen, USA), and RNAse free water to a final volume of 10 µL were mixed before amplification. Validation of differentially transcribed genes and gene expression analyses were performed in StepOne™ Real-Time PCR System (Applied Biosystems).

Quantitative real time PCR

Gene expression analyses were carried out in a StepOne™ Real-Time PCR System (Applied Biosystems) using LuminoCt® SYBR® Green qPCR ReadyMix™(Cat No. L6544, Sigma-Aldrich) and LuminoCt® qPCR ReadyMix™ (Cat No. L6669, Sigma-Aldrich). The pre-designed primers (probe included or not included) were purchased from Applied Biosystems and Integrated DNA Technologies. Gene expression levels were expressed relative to *Gapdh* . The complete list of primers is described in Table 1.

Immunohistochemistry and image analysis

Anesthetized mice were perfused via transcardiac puncture with 4% paraformaldehyde (PFA). P0 offspring were not perfused. The brains were dissected and further fixed with 4% PFA overnight at 4° C and cryoprotected. Brains were cut at 20 µm on a cryostat (Leica) and collected into four series in SuperFrost Plus slides (Thermo Fischer) and subsequently stored at -20° C. Selected 20 µm thick sections (one of four sections) throughout the ARC/ME of P21 offspring were blocked in 2% serum in PBS + 0.1% Triton X-100 and incubated with the following primary antibodies: rabbit anti-Fgf10 (1:200; ABN44 Millipore), mouse anti-occludin, mouse anti-vimentin (1:200; sc-373717 Santa Cruz), and mouse anti-IGFbp2 (1:200; sc-365368 Santa Cruz). The primary antibodies were visualized with goat anti-rabbit Alexa Fluor 488, goat anti-mouse Alexa Fluor 488, or donkey anti-mouse Alexa Fluor 568 (1:300; Life Technologies). Nuclei were counterstained using DAPI. Images were obtained in a Leica laser scanning Confocal Microscope.

AgRP and α-MSH immunohistochemistry and fiber density quantitative analysis

Selected 20 µm thick sections (one of four sections) throughout the ARC/ME of P21 offspring were blocked with 2% chicken serum in KPBS + 0.4% Triton X-100 and incubated with rabbit anti-AGRP antibody (1:500;

Phoenix Pharmaceuticals) or sheep anti-αMSH (1:10.000; Millipore) in blocking solution for 72 hours at 4˚ C. As secondary antibody, a chicken anti-rabbit Alexa Fluor 488 or a donkey anti-sheep Alexa 633 (1:300; Life Technologies) were used. For quantification, representative sections through the PVH (bregma between -0.59 mm and -1.23 mm) and ARC (bregma between -1.43 mm and -1.91 mm) of each animal were acquired using a Leica laser scanning Confocal Microscope. Ten image stacks with 1 μm distance interval throughout the PVH and ARC of each animal were taken. AGRP and α-MSH fiber density analysis was then performed using ImageJ Launcher and based on previously published reports (5, 21). Briefly, each single image was binarized to compensate for differences in fluorescence intensity, specified in a random 200 x 200 μm region and skeletonized, so that each fiber segment was 1 pixel thick. The integrated intensity was then measured for each image. The total density value was obtained by the sum of all image planes analyzed.

Electron microscopy

P0 and P21 offspring mice were perfused with lanthanum and their brains were processed for immunolabeling for electron microscopy examination. Ultrathin sections were then cut on a ultramicrotome, collected on Formvar-coated single-slot grids, and analyzed with a Tecnai 12 BioTWIN electron microscope (FEI).

Statistical analysis

All values were expressed as means ± SEM. Two-group one-factor comparisons were performed using a two-tailed unpaired Student's *t*-test. Four-group two-factor comparisons were performed using two-way ANOVA followed by Tukey's multiple-comparison test when computing confidence intervals for every comparison, or the Holm–Šídák test when not. Analysis was performed with GraphPad v8. Statistical significance was considered $p < 0.05$.

Results

The metabolic phenotype of the offspring of diet-induced obese mothers

To corroborate the effects of maternal diet-induced obesity on offspring metabolic health, six-week-old female mice were fed either Chow or a high-fat diet (HFD) for 4 weeks prior to mating and throughout gestation and lactation (Fig. 1A). As expected, HFD females gained more weight than those kept on Chow (Fig. 1B-1C). DIO offspring were lighter at birth (P0) (Fig. 1D); however, at weaning (P21), the offspring from HFD dams were heavier than controls (Fig. 1E). In addition, they presented systemic glucose intolerance and hyperglycemia (Fig. 1F–1G). These results confirm that maternal DIO alters offspring glucose homeostasis during perinatal life.

Maternal diet-induced obesity disrupts the structure of offspring ME-BBB

We next assessed whether maternal obesogenic environment was sufficient to induce alterations in ME-BBB structure in the offspring. Transmission electron microscopy revealed that blood vessels at the ME/ARC interface were leakier in the offspring of DIO mothers as compared to the offspring of lean mothers (Fig. 2A–2B). The damage in barrier integrity could be seen by the detection of lanthanum outside the capillaries surrounding ARC neurons (see arrowheads in Fig. 2B',2B'', 2B''') in the offspring of mother exposed to HFD, while control offspring showed preserved structure of the BBB (see arrowheads and asterisks in Fig. 2A',2A'', 2A'''). Using an RNA array for transcripts encoding proteins involved in hypothalamic and BBB structure and function (Fig. 3A–3B), we identified several transcripts that were significantly affected by gestational obesity. At birth, DIO offspring presented approximately 50% modulation in the expression of genes related to tight junctions and angiogenesis (Fig. 3A; Table 2). Notwithstanding, at weaning, the majority of the transcript's expression was normalized, except for *Actn3*, *Cldn6,* and *Cldn16* (Fig. 3B; Table 3). In addition, at P0 (Suppl. Fig. 1), several hypothalamic neurotransmitters showed a reduction in expression in the offspring of DIO dams, including *Agrp*, *Drd2*, *Pmch*, *Crh*, and *Trh* (Suppl. Fig. 1B), as well as the tanycytes/BBB transcripts *Glast* and *Msfd2a* (Suppl. Fig. 1C). At weaning, the developmental transcript *Nkx2.2* was increased, whereas *Wnt7a* was decreased (Fig. 3C); the anorexigenic neurotransmitters *Pomc* and *Cart*, as well as the dopamine receptor 2 (*Drd2*), were upregulated (Fig. 3D). The transcripts encoding for tanycyte proteins *Glast* and *Igfbp2* were increased, whereas *Msfd2a*, a gene critical for BBB formation and function, was reduced (Fig. 3E). Moreover, the

transcripts encoding for cytokines *Tnfα*, *Il10,* and *Il6* were increased in the ME-ARC interface in the ofsspring of DIO dams (Fig. 3F).

Cross-fostering from birth to weaning rescues the metabolic impairments led by intrauterine obesogenic exposure

Previous studies have demonstrated the importance of the lactation period on the development of POMC and AgRP neurons (42). To test the hypothesis that breastfeeding on lean mothers could provide a beneficial impact on the ME-BBB abnormalities found in the offspring of DIO mothers, we submitted the newborn mice to a cross-fostering protocol as depicted in Fig. 4A. As a result of the protocol design, we obtained four groups: (1) gestation and lactation by lean dams (COCL); (2) gestation by lean dams and lactation by DIO dams (COHL); (3) gestation by DIO dams and lactation by lean dams (HOCL); (4) gestation and lactation by DIO dams (HOHL) (Fig. 4B). At weaning, offspring exposed to an obesogenic environment during gestation and lactation (HOHL) were heavier, glucose intolerant, and presented greater fasting glucose levels as compared with the offspring of all other three groups (Fig. 4C–E). Of note, lactation by lean mothers reversed the effects of gestational obesogenic development (Fig. 4C–4E) while exclusive breastfeeding on DIO mothers (COHL) was sufficient to induce a tendency of greater body weight and greater fasting blood glucose in the offspring (Fig. 4C–4E).

Cross-fostering during breastfeeding restores the structural organization of the hypothalamus

The difference in the metabolic phenotype of offspring submitted to cross-fostering from birth to weaning led us to ask how breastfeeding would interfere in the structure of the BBB near the ME. Using confocal microscopy, we showed that, in control offspring (COCL), IGFbp2, a marker of β2-tanycytes, was expressed in cells organized linearly in the interface between the ME and the ARC (Fig. 5A); and occludin, a tight-junction protein present in the endothelial cells, appeared as a fine granular stain organized near the walls of the third ventricle (3V) and in the vicinity of the organized β2-tanycytes (Fig. 5A). Moreover, FGF10, which is present in β2-tanycytes and neurons during early development, was expressed in several cells along the 3V, and in the bodies of tanycytes lining in the 3V walls (Fig. 5E); whereas vimentin, which is expressed in ependymal cells and tanycytes, was detected as fine radial projections from the wall of the

third ventricle but was not clearly co-expressed with FGF10 (Fig. 5E). Conversely, in DIO offspring breastfeeding by DIO mothers (HOHL), there was a complete loss of the lining of β2-tanycytes expressing IGFbp2, which were detected as isolated cells within the ARC, whereas occludin labelling was more intense and dispersed across the MBH, as compared with the control group (Fig. 5D). Moreover, several FGF10 expressing cells co-expressed vimentin, suggesting the appearance of transdifferentiated cells (Fig. 5H). These results show that components of the BBB at the ME undergo severe disorganization upon intrauterine and early postnatal exposure to an obesgenic environment. Control offspring breastfeeding by DIO mothers (COHL), IGFbp2 expressing cells were not lined in the interface between the ME and the ARC, but rather concentrated in the region near the angle of the third ventricle in close vicinity with the granular staining of occludin (Fig. 5B). In addition, there were very few cells expressing FGF10 and the tanycyte projections expressing vimentin presented with a very strong and dense staining near the angle of the third ventricle (Fig. 5F), suggesting that lactation by obese mothers is enough to induce alterations in the structure of the ME-BBB. In the offspring of DIO mothers breastfeeding by lean mothers (HOCL), the number of cells expressing IGFbp2 was greater than in both groups breastfeeding by DIO mothers; moreover, occludin staining appeared near the 3V wall and in between the IGFbp2-expressing cells, in a pattern that was similar to the one seen in the control group (Fig. 5C). Finally, the number and distribution of FGF10 expressing cells in HOCL was similar to the control group, as well as the thin and radial vimentin projections towards the ARC (Fig. 5G). This vimentin rearrangement took place despite its dense labeling in the proximity of the 3V wall, as in the hypothalamus of control offspring breastfeeding by DIO mothers, suggesting that lactation by lean mothers is able to partially revert the disarrangements in the ME-BBB structure derived from intrauterine development in an obesogenic environment.

Impact of cross-fostering on AgRP and α-MSH projections

Neurons from the melanocortin system establish their connectivity with other hypothalamic target areas, including the paraventricular hypothalamus (PVH) during the first 2 weeks of postnatal life (4, 11). Using confocal microscopy, we determined the density of AgRP and α-MSH fiber projections in the ARC and PVH at weaning. As compared with the offspring of lean dams breastfeedin by lean dams (COCL), continuous exposure to an obesogenic environment during gestation and lactation (HOHL; DIO offspring breastfeeding

by DIO dams) presented increased AgRP projections to the PVH and ARC, and reduced α-MSH projections to the PVH and ARC (Fig. 6A–L). Although not significant, exclusive lactation by DIO mothers seems to increase AgRP axonal innervation into the PVH (Fig. 6C, Suppl. Fig. 2A) while offspring from DIO dams breastfeeding by a lean mother seem to partially decrease AgRP fiber density in the PVH (Fig. 6C, Suppl. Fig. 2A), with no major changes in the intra-arcuate projections (Fig. 6F, Suppl. Fig. 2C and 2D), or in α-MSH fiber densities to both the PVH and ARC (Fig. 6I and 6L, Suppl. Fig. 2E-H).

Cross-fostering during lactation partially rescues the expression of genes involved in energy balance and BBB integrity in the hypothalamus

We next assessed the impact of cross-fostering on the expression of genes involved in energy balance and BBB integrity in the hypothalamus. Continuous exposure to an obesogenic environment during intrauterine and perinatal life (HOHL) increased the expression of *Pomc* and *Cart* transcripts (Fig. 7A and 7B). Interestingly, a similar expression pattern was observed in the control offspring breastfeeding by DIO dams (COHL) (Fig. 7A and 7B). Conversely, the expression of both *Pomc* and *Cart* transcripts in the hypothalamus of the DIO offspring breastfeeding by lean dams (HOCL) were similar to controls (COCL) (Fig. 7A and 7B). *Drd2* expression was increased in the hypothalamus of the offspring of DIO mothers breastfeeding by DIO mothers (HOHL), whereas in both the offspring of lean mothers breastfeeding by DIO mothers (COHL) and offspring of DIO mothers breastfeeding by lean mothers (HOCL), *Drd2* expression levels were unaltered (Fig. 7C), suggesting that exposure to DIO exclusively during gestation or lactation is not sufficient to influence *Drd2* expression. The expression of transcripts encoding for the neurodevelopmental protein, Nkx2.2, and the tanycyte proteins *Glast* and *Igfbp2,* were increased in the hypothalamus of DIO offspring breastfeeding by DIO mothers (HOHL) (Fig. 7D-7G); whereas in both the control offspring breastfeeding by DIO mothers (COHL) and DIO offspring breastfeeding by lean mothers (HOCL), the levels of all three transcripts were intermediate (Fig. 7D-7G). Finally, the expression of *Msfd2a*, a key marker for BBB formation and function, was strongly downregulated in the offspring of DIO dams breastfeeding by DIO dams (HOHL) (Fig. 7G). Breastfeeding by DIO mothers (COHL) was sufficient to decrease *Msfd2a* expression to similar levels of HOHL, while cross-fostering of DIO offspring by lean mothers (HOCL) was able to rescue *Msfd2a* transcript levels to control animals (COCL) (Fig. 7G).

Long-term impact of cross-fostering on the structural organization of the mediobasal hypothalamus

Because maternal obesity results in increased risk of adult life metabolic diseases in the offspring (1), we asked whether intrauterine and early postnatal development in an obesogenic environment could promote long-lasting changes in the structure of the ME-ARC interface. Using confocal microscopy, we showed that in the hypothalamus of 120-day old control offspring (COCL; control offspring breastfed in lean mothers), vimentin staining was organized with predominant expression in the dorsal part of the 3V walls, in the ME-ARC interface, and within the ME; projections were radial and thin (Fig. 8A and 8E). In addition, the expression of *Rax*, which predominates in tanycytes and POMC precursors, was evident in the ventral walls of the third ventricle and in cell bodies dispersed across the MBH parenchyma (Fig. 8A). In the DIO offspring breastfeeding by DIO mothers (HOHL), vimentin was expressed in cells all along the lateral walls of the third ventricle with thick radial projections towards the MBH and an intense staining in the ME-ARC interface, which was constituted by thick and disorganized projections (Fig. 8D and 8F). In addition, there was intense co-expression of *Rax* and vimentin, as well as a greater number of cells expressing *Rax* across the ME and MBH parenchyma, as compared with COCL offspring (Fig. 8D). In the control offspring breastfeeding by DIO mothers (COHL) and in the DIO offspring breastfeeding by lean mothers (HOCL), the expression of *Rax* followed a pattern that was similar to control mice (COCL) (Fig. 8B and 8C). Moreover, quantification of vimentin density in the ME-ARC intefrace was higher upon continuous exposure to obesogenic environment during development (HOHL) (Fig. 8G), whereas in the control offspring breastfeeding by DIO mothers (COHL) and in the DIO offspring breastfeeding by lean mothers (HOCL), the density of vimentin in the MBH were not different from control offspring (COCL) (Fig. 8G).

Discussion

In this experimental study, we showed that maternal obesity results in defects in the structure and function of the BBB at the hypothalamic ME-ARC interface, and that cross-fostering during lactation by lean mothers corrects, at least in part, these abnormalities.

In human populations, the increased risk for newborn health problems associated with maternal obesity was first described as early as 1949, in a study that evaluated 5,000 pregnant women (17). Thereafter, a rapidly growing number of studies consolidated this concept showing that health problems are not restricted to the perinatal phase, but extends to the entire life, increasing the risk for obesity, DM2, hypertension, and a number of other medical conditions (23, 25, 43). In order to provide mechanistic advance that could help in preventing and treating the descendant diseases that emerge from maternal obesity, experimental models have been optimized to reproduce much of the outcomes exhibited by humans (39). In nonhuman primates, maternal obesity induced by the consumption of a HFD, resulted in hypothalamic inflammation, which was accompanied by an abnormal development of the melanocortin system (18, 40). Likewise, in mice, maternal obesity promoted hypothalamic inflammation in the offspring, which was characterized by the activation of toll-like receptor-4 signaling, and activation of c-Jun N-terminal kinase 1 and IkB-kinase (37, 41). Thus, it is currently known that, in addition to the well-known impact of maternal obesity on offspring metabolic and cardiovascular health, the hypothalamus is also affected.

In rodents, final development of the melanocortin system occurs postnatally, during the first 2 weeks after birth (4, 6). Disturbances during this critical developmental window alters the organization of AgRP and POMC axonal projections and increases the offspring susceptibility to develop obesity and DM2 in both mice and nonhuman primates (34, 42). These data support the importance of postnatal nutrition on hypothalamic programming. Here, we add important information to this concept by showing that lactation by DIO dams, can not only disturb POMC and AgRP axonal projections to the paraventricular hypothalamus, but it is also sufficient to modulate the expression of *Pomc* and *Cart*. Moreover, cross-fostering by lean mothers during lactation is sufficient to prevent the impact of HFD on melanocortin projection development, as well as to revert the defective expression of these neuropeptides. Of note, we have observed an increase in AgRP fiber density reaching the PVH, opposing to what has been reported in previous studies (34, 42). We identified two factors that could explain the difference: i, in our study, analysis was performed at weaning, whereas in the other two studies, analysis occurred during adulthood; ii, in addition, there were differences in diet composition, particularly the amount of fat and carbohydrates

342 and also there were differences in the protocol of maternal nutritional intervention. Thus, in the future,
343 studies could be designed to explore in detail these factors.

344 Tanycytes are regarded as the gatekeepers that directly control the transport of nutrients to
345 neurons (28, 35). We show that maternal obesity induces a disruption in ME-BBB integrity, which is
346 accompanied by abnormal distribution of tanycytes, increased vimentin fibers, and rupture of the BBB
347 capilaries. Integrity of the BBB was evaluated using the gold-standard transmission electron microscopy in
348 mice perfused with lanthanum (8). The results provide evidence for the disruption of the BBB in the
349 offspring of obese mothers, which was further confirmed by gene expression and structural analysis. These
350 data support the idea that intrauterine and postnatal exposure to an obesogenic environment might
351 primarily affect BBB development (as seen by over 50% modulation in tight junction and angiogenesis
352 genes at birth). This defective BBB integrity might consequently induce a disarrangement in tanycytic
353 organization throughout the third ventricle wall, contributing to BBB leakage and impacting the access of
354 blood-borne signals to the brain parenchyma close to the ARC-adjacent neurons. Subsequent alterations in
355 neuronal uptake of nutrients, inflammation, and impaired development of the mediobasal hypothalamus,
356 may lead to impaired control of energy homeostasis. The possibility to partially restore ME-BBB structure
357 during breastfeeding provides a preventive strategy of nutritional intervention during early life.

358 In addition to the anatomical data showing that maternal obesity disrupts the structure of the ME-
359 BBB, our molecular studies show a striking reduction in *Mfsd2a* transcript. Interestingly, *Mfsd2a* has been
360 shown to be essential for BBB structure and function (3, 33). Our results show that cross-fostering of DIO
361 offspring by lean dams can restore the alterations in *Mfsd2a* transcript, while cross-fostering of chow
362 offspring by obese dams is enough to downregulate *Mfsd2a* expression. This supports the importance of
363 the lactation period on barrier integrity and plasticity and strengthens the possibility for nutritional
364 interventions during early life as possible preventive measures against obesogenic exposure during
365 intrauterine life.

366 As this was an exploratory study, we decided to evaluate only the male offspring; however,
367 considering the possibility of the existance of a sexual dimorphism in the defects herein reported, we

acknowledge that this could be regarded as a weakness of the study, and we propose that in future studies, female offspring should also be evaluated.

Collectively, our study strengthens the idea of the importance of the lactation period for proper development of the mediobasal hypothalamus. The developing central nervous system during perinatal life retains plasticity capacities that enable recovery from the damage occasioned from obesogenic gestational development. Therefore, preventive nutritional strategies during breastfeeding can counteract the negative impacts of maternal obesity. On the other side, it is also important to raise awareness that nutritional care should continue throughout gestation and lactation, since lactation by obese mothers per se can have some detrimental effects on barrier permeability and consequential metabolic outcomes in the offspring.

In conclusion, our study provides evidence that cross-fostering during lactation by lean dams can improve the abnormalities of ME-BBB structure and function produced by the exposure to an obesogenic environment during gestation; and this can positively impact the metabolic outcomes in the progeny. Nutritional interventions during breastfeeding (maternal diet or milk donations from healthy mothers) might account for a social health strategy that can improve the quality of life of future generations.

Acknowledgements

We are grateful to Erika Roman, Marcio Cruz, and Gerson Ferraz for laboratory management.

Funding

This study was funded by the Sao Paulo Research Foundation (2013/07607-8) and the National Institute of Science and Technology (Neuroimmunomodulation) (to L.A.V.); Sao Paulo Research Foundation postdoctoral fellowship (2015/02913-9) and a Marie Skłodowska-Curie Action fellowship under the European Union's Horizon 2020 research and innovation programme (H2020-MSCA-IF) NEUROPREG (grant agreement no. 891247) (to R.H-T.).

Disclosure

The authors declare no competing interests.

Author contributions

R.H.-T. and L.A.V. conceptualized and supervised the study. L.A.V. administered the project and acquired project funding. R.H.-T., J.M., V.C.D.B., R.S.C., C.S., N.R.D. performed experiments and discussed data. R.B. performed electron microscopy data acquisition and analyses. R.H.-T., J.M. and L.A.V. contributed to method development and data interpretation. R.H.-T. and L.A.V. developed the data visualizations. R.H.-T. and L.A.V. wrote the original draft of the paper with editing and reviewing inputs from all authors.

References

1. **Ainge H, Thompson C, Ozanne SE, and Rooney KB**. A systematic review on animal models of maternal high fat feeding and offspring glycaemic control. *Int J Obes (Lond)* 35: 325-335, 2011.
2. **Balland E, Dam J, Langlet F, Caron E, Steculorum S, Messina A, Rasika S, Falluel-Morel A, Anouar Y, Dehouck B, Trinquet E, Jockers R, Bouret SG, and Prevot V**. Hypothalamic tanycytes are an ERK-gated conduit for leptin into the brain. *Cell Metab* 19: 293-301, 2014.
3. **Ben-Zvi A, Lacoste B, Kur E, Andreone BJ, Mayshar Y, Yan H, and Gu C**. Mfsd2a is critical for the formation and function of the blood-brain barrier. *Nature* 509: 507-511, 2014.
4. **Bouret SG**. Developmental programming of hypothalamic melanocortin circuits. *Exp Mol Med* 54: 403-413, 2022.
5. **Bouret SG, Draper SJ, and Simerly RB**. Formation of projection pathways from the arcuate nucleus of the hypothalamus to hypothalamic regions implicated in the neural control of feeding behavior in mice. *J Neurosci* 24: 2797-2805, 2004.
6. **Bouret SG, Draper SJ, and Simerly RB**. Trophic action of leptin on hypothalamic neurons that regulate feeding. *Science* 304: 108-110, 2004.
7. **Bouret SG, Gorski JN, Patterson CM, Chen S, Levin BE, and Simerly RB**. Hypothalamic neural projections are permanently disrupted in diet-induced obese rats. *Cell Metab* 7: 179-185, 2008.
8. **Butt AM, Jones HC, and Abbott NJ**. Electrical resistance across the blood-brain barrier in anaesthetized rats: a developmental study. *J Physiol* 429: 47-62, 1990.
9. **Chen N, Zhang Y, Wang M, Lin X, Li J, Li J, and Xiao X**. Maternal obesity interrupts the coordination of the unfolded protein response and heat shock response in the postnatal developing hypothalamus of male offspring in mice. *Mol Cell Endocrinol* 527: 111218, 2021.
10. **Clarke IJ**. Hypothalamus as an endocrine organ. *Compr Physiol* 5: 217-253, 2015.

11. **Coupe B, and Bouret SG**. Development of the hypothalamic melanocortin system. *Front Endocrinol (Lausanne)* 4: 38, 2013.

12. **Croizier S, and Bouret SG**. Molecular control of the development of hypothalamic neurons involved in metabolic regulation. *J Chem Neuroanat* 123: 102117, 2022.

13. **De Souza CT, Araujo EP, Bordin S, Ashimine R, Zollner RL, Boschero AC, Saad MJ, and Velloso LA**. Consumption of a fat-rich diet activates a proinflammatory response and induces insulin resistance in the hypothalamus. *Endocrinology* 146: 4192-4199, 2005.

14. **Dearden L, Buller S, Furigo IC, Fernandez-Twinn DS, and Ozanne SE**. Maternal obesity causes fetal hypothalamic insulin resistance and disrupts development of hypothalamic feeding pathways. *Mol Metab* 42: 101079, 2020.

15. **Engel DF, and Velloso LA**. The timeline of neuronal and glial alterations in experimental obesity. *Neuropharmacology* 208: 108983, 2022.

16. **Ganong WF**. Circumventricular organs: definition and role in the regulation of endocrine and autonomic function. *Clin Exp Pharmacol Physiol* 27: 422-427, 2000.

17. **Gilbert JA**. The association of maternal obesity, large babies, and diabetes. *Br Med J* 1: 702-704, 1949.

18. **Grayson BE, Levasseur PR, Williams SM, Smith MS, Marks DL, and Grove KL**. Changes in melanocortin expression and inflammatory pathways in fetal offspring of nonhuman primates fed a high-fat diet. *Endocrinology* 151: 1622-1632, 2010.

19. **Guillebaud F, Duquenne M, Djelloul M, Pierre C, Poirot K, Roussel G, Riad S, Lanfray D, Morin F, Jean A, Tonon MC, Gaige S, Lebrun B, Dallaporta M, Leprince J, Prevot V, and Troadec JD**. Glial Endozepines Reverse High-Fat Diet-Induced Obesity by Enhancing Hypothalamic Response to Peripheral Leptin. *Mol Neurobiol* 57: 3307-3333, 2020.

20. **Haan N, Goodman T, Najdi-Samiei A, Stratford CM, Rice R, El Agha E, Bellusci S, and Hajihosseini MK**. Fgf10-expressing tanycytes add new neurons to the appetite/energy-balance regulating centers of the postnatal and adult hypothalamus. *J Neurosci* 33: 6170-6180, 2013.

21. **Haddad-Tovolli R, Altirriba J, Obri A, Sanchez EE, Chivite I, Mila-Guasch M, Ramirez S, Gomez-Valades AG, Pozo M, Burguet J, Velloso LA, and Claret M**. Pro-opiomelanocortin (POMC) neuron translatome signatures underlying obesogenic gestational malprogramming in mice. *Mol Metab* 36: 100963, 2020.

22. **Haddad-Tovolli R, Dragano NRV, Ramalho AFS, and Velloso LA**. Development and Function of the Blood-Brain Barrier in the Context of Metabolic Control. *Front Neurosci* 11: 224, 2017.

23. **Heslehurst N, Vieira R, Akhter Z, Bailey H, Slack E, Ngongalah L, Pemu A, and Rankin J**. The association between maternal body mass index and child obesity: A systematic review and meta-analysis. *PLoS Med* 16: e1002817, 2019.

24. **Jiang H, Gallet S, Klemm P, Scholl P, Folz-Donahue K, Altmuller J, Alber J, Heilinger C, Kukat C, Loyens A, Muller-Fielitz H, Sundaram S, Schwaninger M, Prevot V, and Bruning JC**. MCH Neurons Regulate Permeability of the Median Eminence Barrier. *Neuron* 107: 306-319 e309, 2020.

25. **Kankowski L, Ardissino M, McCracken C, Lewandowski AJ, Leeson P, Neubauer S, Harvey NC, Petersen SE, and Raisi-Estabragh Z**. The Impact of Maternal Obesity on Offspring Cardiovascular Health: A Systematic Literature Review. *Front Endocrinol (Lausanne)* 13: 868441, 2022.

26. **Kim DW, Glendining KA, Grattan DR, and Jasoni CL**. Maternal Obesity in the Mouse Compromises the Blood-Brain Barrier in the Arcuate Nucleus of Offspring. *Endocrinology* 157: 2229-2242, 2016.

27. **Lama A, Pirozzi C, Severi I, Morgese MG, Senzacqua M, Annunziata C, Comella F, Del Piano F, Schiavone S, Petrosino S, Mollica MP, Diano S, Trabace L, Calignano A, Giordano A, Mattace Raso G, and Meli R**. Palmitoylethanolamide dampens neuroinflammation and anxiety-like behavior in obese mice. *Brain Behav Immun* 102: 110-123, 2022.

28. **Langlet F**. Tanycyte Gene Expression Dynamics in the Regulation of Energy Homeostasis. *Front Endocrinol (Lausanne)* 10: 286, 2019.

29. **Langlet F, Mullier A, Bouret SG, Prevot V, and Dehouck B**. Tanycyte-like cells form a blood-cerebrospinal fluid barrier in the circumventricular organs of the mouse brain. *J Comp Neurol* 521: 3389-3405, 2013.

30. **Lee DA, Bedont JL, Pak T, Wang H, Song J, Miranda-Angulo A, Takiar V, Charubhumi V, Balordi F, Takebayashi H, Aja S, Ford E, Fishell G, and Blackshaw S**. Tanycytes of the hypothalamic median eminence form a diet-responsive neurogenic niche. *Nat Neurosci* 15: 700-702, 2012.

31. **Milanski M, Degasperi G, Coope A, Morari J, Denis R, Cintra DE, Tsukumo DM, Anhe G, Amaral ME, Takahashi HK, Curi R, Oliveira HC, Carvalheira JB, Bordin S, Saad MJ, and Velloso LA**. Saturated fatty acids produce an inflammatory response predominantly through the activation of TLR4 signaling in hypothalamus: implications for the pathogenesis of obesity. *J Neurosci* 29: 359-370, 2009.

32. **Mullier A, Bouret SG, Prevot V, and Dehouck B**. Differential distribution of tight junction proteins suggests a role for tanycytes in blood-hypothalamus barrier regulation in the adult mouse brain. *J Comp Neurol* 518: 943-962, 2010.

33. **Nguyen LN, Ma D, Shui G, Wong P, Cazenave-Gassiot A, Zhang X, Wenk MR, Goh EL, and Silver DL**. Mfsd2a is a transporter for the essential omega-3 fatty acid docosahexaenoic acid. *Nature* 509: 503-506, 2014.

34. **Park S, Jang A, and Bouret SG**. Maternal obesity-induced endoplasmic reticulum stress causes metabolic alterations and abnormal hypothalamic development in the offspring. *PLoS Biol* 18: e3000296, 2020.

35. **Prevot V, Dehouck B, Sharif A, Ciofi P, Giacobini P, and Clasadonte J**. The Versatile Tanycyte: A Hypothalamic Integrator of Reproduction and Energy Metabolism. *Endocr Rev* 39: 333-368, 2018.

36. **Ramalho AF, Bombassaro B, Dragano NR, Solon C, Morari J, Fioravante M, Barbizan R, Velloso LA, and Araujo EP**. Dietary fats promote functional and structural changes in the median eminence blood/spinal fluid interface-the protective role for BDNF. *J Neuroinflammation* 15: 10, 2018.

37. **Rother E, Kuschewski R, Alcazar MA, Oberthuer A, Bae-Gartz I, Vohlen C, Roth B, and Dotsch J**. Hypothalamic JNK1 and IKKbeta activation and impaired early postnatal glucose metabolism after maternal perinatal high-fat feeding. *Endocrinology* 153: 770-781, 2012.

38. **Schaeffer M, Langlet F, Lafont C, Molino F, Hodson DJ, Roux T, Lamarque L, Verdie P, Bourrier E, Dehouck B, Baneres JL, Martinez J, Mery PF, Marie J, Trinquet E, Fehrentz JA, Prevot V, and Mollard P**. Rapid sensing of circulating ghrelin by hypothalamic appetite-modifying neurons. *Proc Natl Acad Sci U S A* 110: 1512-1517, 2013.

39. **Schoonejans JM, and Ozanne SE**. Developmental programming by maternal obesity: Lessons from animal models. *Diabet Med* 38: e14694, 2021.

40. **Sullivan EL, Rivera HM, True CA, Franco JG, Baquero K, Dean TA, Valleau JC, Takahashi DL, Frazee T, Hanna G, Kirigiti MA, Bauman LA, Grove KL, and Kievit P**. Maternal and postnatal high-fat diet consumption programs energy balance and hypothalamic melanocortin signaling in nonhuman primate offspring. *Am J Physiol Regul Integr Comp Physiol* 313: R169-R179, 2017.

41. **Velloso LA**. Maternal consumption of high-fat diet disturbs hypothalamic neuronal function in the offspring: implications for the genesis of obesity. *Endocrinology* 153: 543-545, 2012.

42. **Vogt MC, Paeger L, Hess S, Steculorum SM, Awazawa M, Hampel B, Neupert S, Nicholls HT, Mauer J, Hausen AC, Predel R, Kloppenburg P, Horvath TL, and Bruning JC**. Neonatal insulin action impairs hypothalamic neurocircuit formation in response to maternal high-fat feeding. *Cell* 156: 495-509, 2014.

43. **Warrington NM, Beaumont RN, Horikoshi M, Day FR, Helgeland O, Laurin C, Bacelis J, Peng S, Hao K, Feenstra B, Wood AR, Mahajan A, Tyrrell J, Robertson NR, Rayner NW, Qiao Z, Moen GH, Vaudel M, Marsit CJ, Chen J, Nodzenski M, Schnurr TM, Zafarmand MH, Bradfield JP, Grarup N, Kooijman MN, Li-Gao R, Geller F, Ahluwalia TS, Paternoster L, Rueedi R, Huikari V, Hottenga JJ, Lyytikainen LP, Cavadino A, Metrustry S, Cousminer DL, Wu Y, Thiering E, Wang CA, Have CT, Vilor-Tejedor N, Joshi PK, Painter JN, Ntalla I, Myhre R, Pitkanen N, van Leeuwen EM, Joro R, Lagou V, Richmond RC, Espinosa A, Barton SJ, Inskip HM, Holloway JW, Santa-Marina L, Estivill X, Ang W, Marsh JA, Reichetzeder C, Marullo L, Hocher B, Lunetta KL, Murabito JM, Relton CL, Kogevinas M, Chatzi L, Allard C, Bouchard L, Hivert MF, Zhang G, Muglia LJ, Heikkinen J, Consortium EGG, Morgen CS, van Kampen AHC, van Schaik BDC, Mentch FD, Langenberg C, Luan J, Scott RA, Zhao JH, Hemani G, Ring SM, Bennett AJ, Gaulton KJ, Fernandez-Tajes J, van Zuydam NR, Medina-Gomez C, de Haan HG, Rosendaal FR, Kutalik Z, Marques-Vidal P, Das S, Willemsen G, Mbarek H, Muller-Nurasyid M, Standl M, Appel EVR, Fonvig CE, Trier C, van Beijsterveldt CEM, Murcia M, Bustamante M, Bonas-Guarch S, Hougaard DM, Mercader JM, Linneberg A, Schraut KE, Lind PA, Medland SE, Shields BM, Knight BA, Chai JF, Panoutsopoulou K, Bartels M, Sanchez F, Stokholm J, Torrents D, Vinding RK, Willems SM, Atalay M, Chawes BL, Kovacs P, Prokopenko I, Tuke MA, Yaghootkar H, Ruth KS, Jones SE, Loh PR, Murray A, Weedon MN, Tonjes A, Stumvoll M, Michaelsen KF, Eloranta AM, Lakka TA, van Duijn CM, Kiess W, Korner A, Niinikoski H, Pahkala K, Raitakari OT, Jacobsson B, Zeggini E, Dedoussis GV, Teo YY, Saw SM, Montgomery GW, Campbell H, Wilson JF, Vrijkotte TGM, Vrijheid M, de Geus E, Hayes MG, Kadarmideen HN, Holm JC, Beilin LJ, Pennell CE, Heinrich J, Adair LS, Borja JB, Mohlke KL, Eriksson JG, Widen EE, Hattersley AT, Spector TD, Kahonen M, Viikari JS, Lehtimaki T, Boomsma DI, Sebert S, Vollenweider P, Sorensen TIA, Bisgaard H, Bonnelykke K, Murray JC, Melbye M, Nohr EA, Mook-Kanamori DO, Rivadeneira F, Hofman A, Felix JF, Jaddoe VWV, Hansen T, Pisinger C, Vaag AA, Pedersen O, Uitterlinden AG, Jarvelin MR, Power C, Hypponen E, Scholtens DM, Lowe WL, Jr., Davey Smith G, Timpson NJ, Morris AP, Wareham NJ, Hakonarson H, Grant SFA, Frayling TM, Lawlor DA, Njolstad PR, Johansson S, Ong KK, McCarthy MI, Perry JRB, Evans DM, and Freathy RM**. Maternal and fetal genetic effects on birth weight and their relevance to cardio-metabolic risk factors. *Nat Genet* 51: 804-814, 2019.

44. **Weindl A, and Joynt RJ**. Barrier properties of the subcommissural organ. *Arch Neurol* 29: 16-22, 1973.

554

555

Figure legends

Fig. 1 | **Maternal HFD affects offspring physiology at weaning. (A)** Experimental design of maternal dietary conditions and offspring collection. **(B)** Maternal body weight gain throughout the experimental studies (n=5 per group). **(C)** Female body weight gain at the onset of pregnancy (after 4 weeks in HFD) (n= 5 per group). **(D-E)** Body weight differences between P0 **(D)** and P21 **(E)** Chow and HFD offspring (n=9-20 per group). **(F)** Glucose tolerance test and area under the curve (AUC) of P21 Chow and HFD male offspring (n=10 per group). **(G)** Blood glucose levels of P21 Chow and HFD male offspring after 6 h of fasting (n=10 per group). Dots in all panels represent individual sample data. Data are expressed as the mean ± SEM. *p < 0.05; **p < 0.01; ***p < 0.001 ****p < 0.0001.

Fig. 2 | **Maternal HFD disrupts the structure of the blood-brain barrier at the interface of the median eminence.** Representative electron micrographs of the BBB/ME interface in the arcuate nucleus of the hypothalamus of Chow **(A-C)** and HFD **(D-F)** P21 male offspring (n=3 per group; representative images shown of one animal per group). **(A')** Blood capillaries surrounding the perfused lanthanum (see arrows). **(A''-A''')** Images show intact hypothalamic parenchima and ARC neurons (see asterisks). **(B')** BBB disruption observed by the leakage of the tracer into the neural tissue (see arrow). **(B''-B''')** Images show the presence of tracer aggregates (black arrows) in the cytoplasm of ARC neurons (asterisks).

Fig. 3 | **Gene expression profile of tight junctions, developmental, hypothalamic neurotransmitters and inflammation after maternal HFD exposure at weaning. (A-B)** PCR array of main tight junctions, adhesion and angiogenesis genes involved in BBB structure and function showing upregulated (red) and downregulated genes (green) in P0 **(A)** and P21 **(B)** upon maternal HFD exposure (HFD-O vs. Chow-O) (n=5 per group). Significance was considered upon fold change above ± 2.0 and p < 0.05. **(C-F)** Transcript expression of genes involved in neuronal development, axonal guidance and angiogenesis **(C)**, main hypothalamic neurotransmitters **(D)**, glial markers **(E)**, and inflammatory markers **(F)** P21 male offspring of HFD dams (HFD-O vs. Chow-O) (n=5-6 per group). Dots in all panels represent individual sample data. Data

are expressed as the mean ± SEM. *p < 0.05; **p < 0.01; ***p < 0.001. *Nkx2.2:* NK2 Homeobox 2; *Sox2:* SRY-box 2; *Tgfβ:* transforming growth factor-beta; *Shh:* Sonic Hedgehog; *Bmp7:* Bone morphogenetic proteins; *Wnt5a:* Wnt Family Member 5a; *Wnt7a:* Wnt Family Member 7a; *Wnt7b:* Wnt Family Member 7b; *Vegf:* Vascular endothelial growth factor; *Ang:* angiotensin; *Angpt1:* angiopoietin 1; *Edn1:* Endothelin 1; *Npy:* neuropeptide Y*; Agrp*: agouti-related peptide; *Pomc:* pro-opiomelanocortin; *Cart:* cocaine- and amphetamine-regulated transcript; *Th:* tyrosine hydroxylase; *Drd2:* dopamine receptor 2; *Pmch:* pro-melanin concentrating hormone; *Crh:* corticotropin releasing hormone; *Trh:* Thyrotropin Releasing Hormone; *Glast:* Solute Carrier Family 1Member 3; *Glut:* Solute Carrier Family 2 Member 1; *Fgf10:* Fibroblast Growth Factor 10; *Igfbp2:* Insulin Like Growth Factor Binding Protein 2; *Cav:* caveolin; *Gfap:* Glial Fibrillary Acidic Protein*; Igf1:* Insulin Like Growth Factor 1; *Msfd2a:* Major Facilitator Superfamily Domain Containing 2A; *Tnfα:* Tumor Necrosis Factor; *Il10:* Interleukin 10; *Il6:* Interleukin 6; *Il1β:* Interleukin 1 Beta; *Cd11b:* integrin Subunit Alpha M; *Cx3cl1:*C-X3-C Motif Chemokine Ligand 1.

Fig. 4 | **Cross-fostering is sufficient to rescue physiological impairments led by intrauterine obesogenic exposure. (A-B)** Experimental design of maternal cross-fostering from birth to weaning **(A)** leading to four experimental groups: intrauterine development in Chow environment (CO) and lactation either by Chow dam (COCL) or HFD dam (COHL) and intrauterine development in obesogenic environment (HO) and lactation either by Chow dam (HOCL) or HFD dam (HOHL) **(B)**. **(C)** Body weight differences at weaning (n=6-10 per group). **(D)** Glucose tolerance test and area under the curve (AUC) of P21 male offspring in each of the 4 groups obtained (n=6-10 per group). **(E)** Blood glucose levels after 6 h of fasting of P21 male offspring in each of the 4 groups obtained (n=6-10 per group). Dots in all panels represent individual sample data. Data are expressed as the mean ± SEM. *p < 0.05; **p < 0.01; ***p < 0.001 ****p < 0.0001.

Fig. 5 | **Cross-fostering restores BBB integrity. (A-D)** Representative confocal images of occludin (red) and Igfbp2 (green) expression in the ME/ARC of Chow **(A)** and HFD **(D)** offspring that were cross-fostered during lactation by HFD **(B)** or Chow **(C)** dams. Nuclei are stained with DAPI (blue). **(E-H)** Representative confocal

images of vimentin (red) and Fgf10 (green) expression in the ME/ARC of Chow **(E)** and HFD **(H)** offspring that were cross-fostered during lactation by HFD **(F)** or Chow **(G)** dams. Nuclei are stained with DAPI (blue). Scale bar: 50µm.

Fig. 6 | **Cross-fostering is sufficient to rescue axonal wiring disruptions consequent from intrauterine obesogenic exposure. (A-F)** Representative confocal images of AgRP fibers in the in the PVH **(A-B)** and ARC **(D-E)** of COCL and HOHL P21 offspring and integrated density quantification **(C and F)** (n=3 per group). **(G-L)** Representative confocal images of α-MSH fibers in the in the PVH **(G-H)** and ARC **(J-K)** of COCL and HOHL P21 offspring and integrated density quantification **(I and L)** (n=3 per group). Dots in all panels represent individual sample data. Data are expressed as the mean ± SEM. *p < 0.05. Abbreviations: third ventricle (3V), hypothalamic arcuate nucleus (ARC), hypothalamic paraventricular nucleus (PVH). Scale bar: 100µm.

Fig. 7 | **Cross-fostering is sufficient to rescue gene expression changes induced by intrauterine obesogenic exposure. (A-G)** Transcript expression of *Pomc* **(A)**, *Cart* **(B)**, *Drd2* **(C)**, *Nkx2.2* **(D)**, *Glast* **(E)**, *Igfbp2* **(F)** and *Msfd2a* **(G)** in P21 male offspring of HFD dams (HFD-O vs. Chow-O) (n=5-6 per group). Dots in all panels represent individual sample data. Data are expressed as the mean ± SEM. *p < 0.05; **p < 0.01; ***p < 0.001. *Pomc:* pro-opiomelanocortin; *Cart:* cocaine- and amphetamine-regulated transcript; *Drd2:* dopamine receptor 2; *Nkx2.2:* NK2 Homeobox 2; *Glast:* Solute Carrier Family 1Member 3; *Igfbp2:* Insulin Like Growth Factor Binding Protein 2; *Msfd2a:* Major Facilitator Superfamily Domain Containing 2A.

Fig. 8 | **Cross-fostering vimentin. (A-F)** Representative confocal images of vimentin fibers (red) in the in the ME/ARC interface of Chow **(A)** and HFD **(D)** offspring that were cross-fostered during lactation ~~in~~ by HFD **(B)** or Chow **(C)** dams. **(E-F)** show higher magnification of **(A)** and **(D)**. Nuclei are stained with DAPI (blue). Scale bar: 100 µm **(A-F)** and 50 µm **(E-F)**. **(G)** Integrated density quantification of vimentin (n=3 per group). Dots in all panels represent individual sample data. Data are expressed as the mean ± SEM. *p < 0.05. Abbreviations: third ventricle (3V).

Supplementary Data can be accessed here: https://doi.org/10.6084/m9.figshare.21769709

Table 1 l Gene names, number of the assays, nucleotide and exon region used for primer design.

Table 2 l Fold Regulation of genes significantly altered in the mediobasal hypothalamus of Chow and HFD male offspring at birth (P0).

Table 3 l Fold Regulation of genes significantly altered in the mediobasal hypothalamus of Chow and HFD male offspring at weaning (P21).

Maternal obesity damages the median eminence blood-brain barrier structure and function in the progeny: The beneficial impact of cross-fostering by lean mothers

METHODS

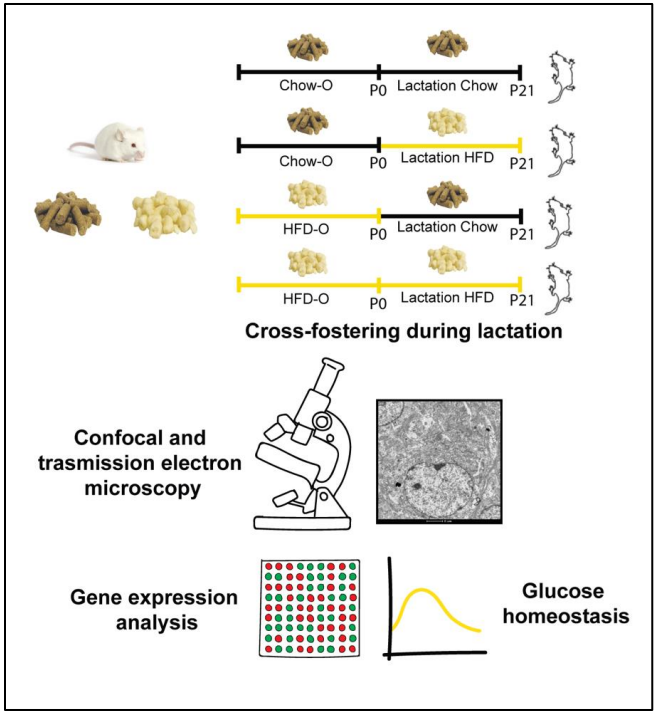

OUTCOME

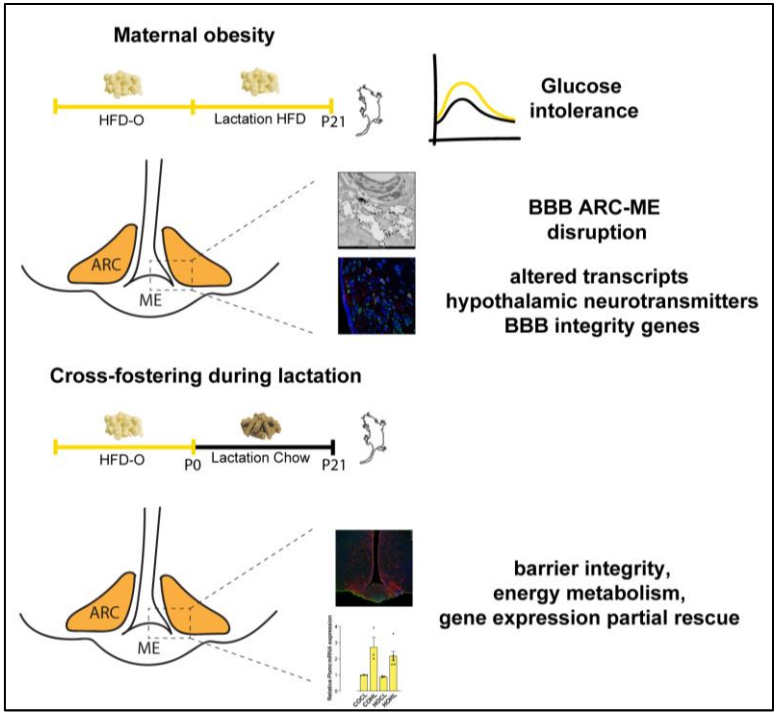

CONCLUSION

Cross-fostering during lactation on lean dams can improve the abnormalities of ME-BBB structure and function produced by the exposure to an obesogenic environment during gestation, with a positive impact the metabolic outcomes in the progeny

Figure 1

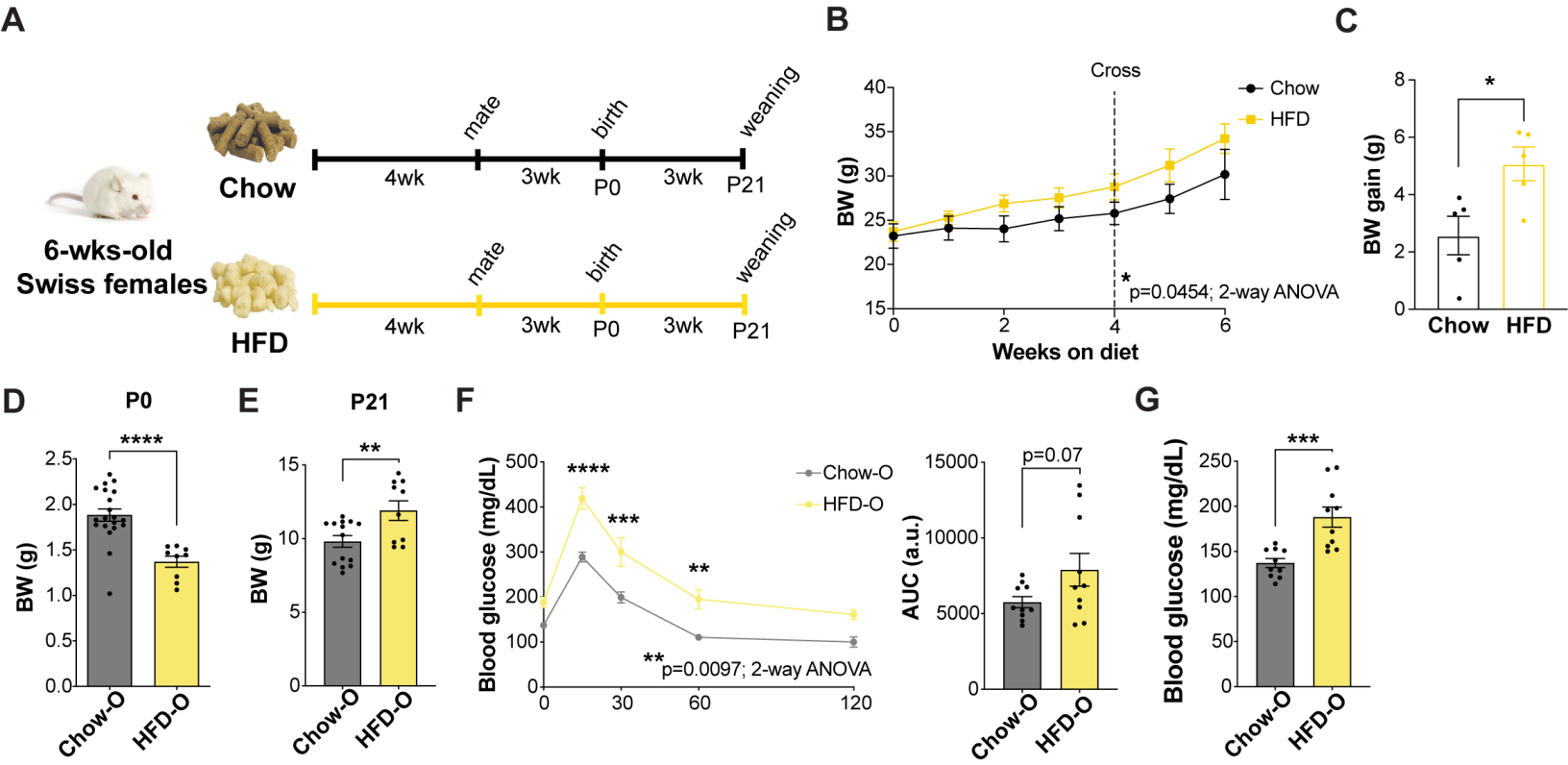
A
6-wks-old
Swiss females
Chow
HFD
mate
birth
weaning
4wk
3wk
P0
3wk
P21
B
Cross
Chow
HFD
BW (g)
Weeks on diet
* p=0.0454; 2-way ANOVA
C
BW gain (g)
*
Chow
HFD
D
P0
BW (g)
****
Chow-O
HFD-O
E
P21
BW (g)
**
Chow-O
HFD-O
F
Blood glucose (mg/dL)
Chow-O
HFD-O
****
***
**
** p=0.0097; 2-way ANOVA
AUC (a.u.)
p=0.07
Chow-O
HFD-O
G
Blood glucose (mg/dL)
***
Chow-O
HFD-O

Figure 2

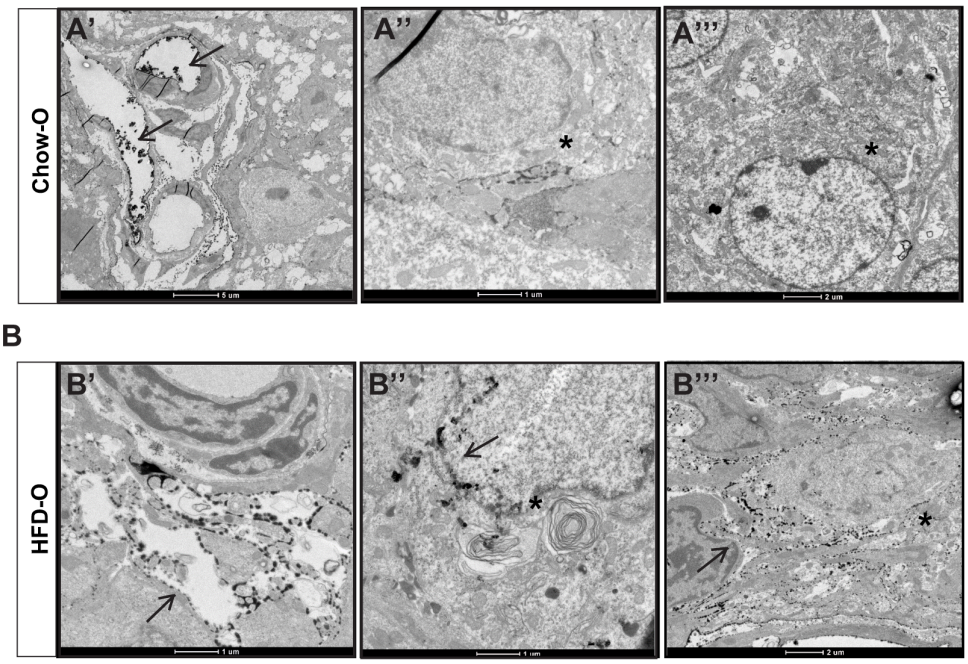

A

Figure 3

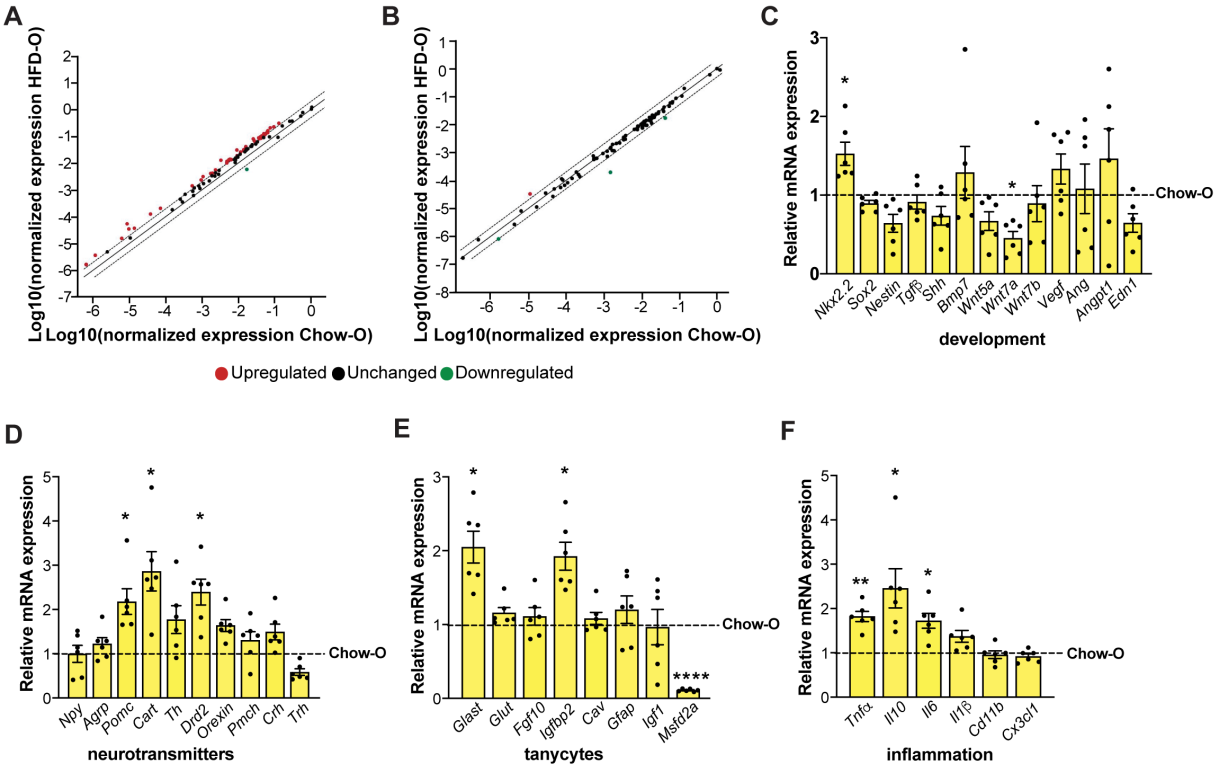
A
B
C
Log10(normalized expression HFD-O)
Log10(normalized expression Chow-O)
Upregulated
Unchanged
Downregulated
Relative mRNA expression
Chow-O
Nkx2.2
Sox2
Nestin
Tgfβ
Shh
Bmp7
Wnt5a
Wnt7a
Wnt7b
Vegf
Ang
Angpt1
Edn1
development
D
E
F
Npy
Agrp
Pomc
Cart
Th
Drd2
Orexin
Pmch
Crh
Trh
neurotransmitters
Glast
Glut
Fgf10
Igfbp2
Cav
Gfap
Igf1
Msfd2a
tanycytes
Tnfα
Il10
Il6
Il1β
Cd11b
Cx3cl1
inflammation

Figure 4

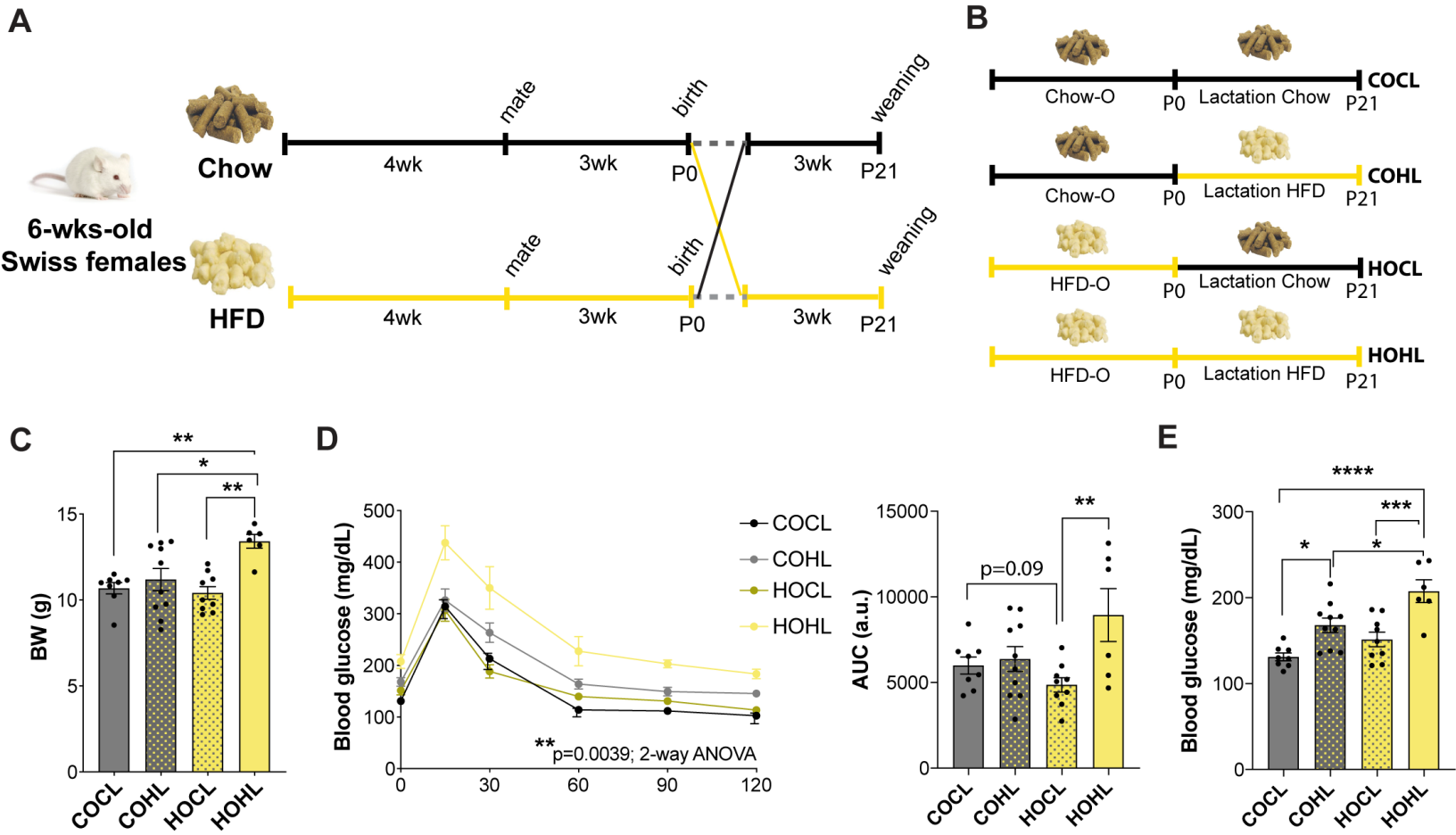
A
Chow
mate
birth
weaning
4wk
3wk
P0
3wk
P21
6-wks-old
Swiss females
HFD
mate
birth
weaning
4wk
3wk
P0
3wk
P21
B
Chow-O
P0
Lactation Chow
P21
COCL
Chow-O
P0
Lactation HFD
P21
COHL
HFD-O
P0
Lactation Chow
P21
HOCL
HFD-O
P0
Lactation HFD
P21
HOHL
C
BW (g)
COCL
COHL
HOCL
HOHL
D
Blood glucose (mg/dL)
COCL
COHL
HOCL
HOHL
** p=0.0039; 2-way ANOVA
AUC (a.u.)
p=0.09
E
Blood glucose (mg/dL)

Figure 5

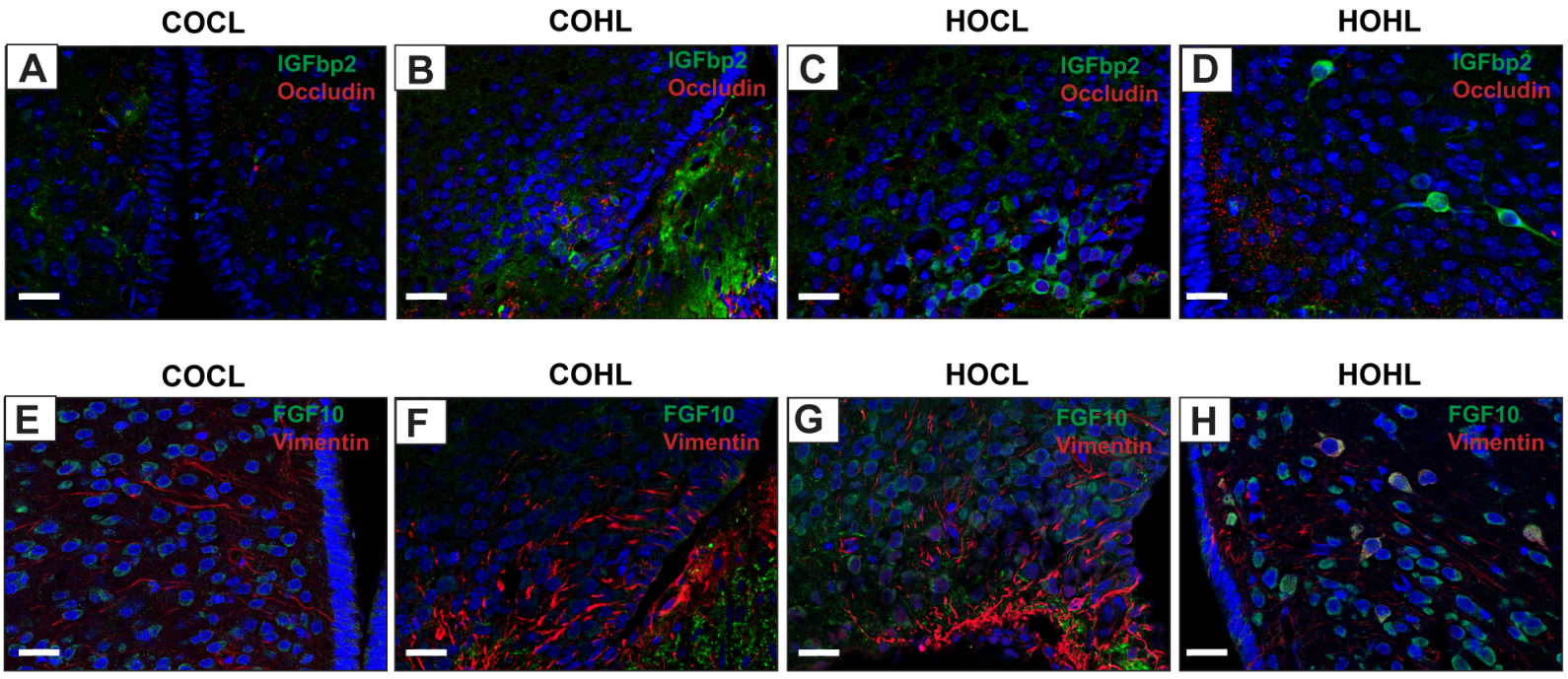
COCL
COHL
HOCL
HOHL
A
IGFbp2
Occludin
B
IGFbp2
Occludin
C
IGFbp2
Occludin
D
IGFbp2
Occludin
COCL
COHL
HOCL
HOHL
E
FGF10
Vimentin
F
FGF10
Vimentin
G
FGF10
Vimentin
H
FGF10
Vimentin

Figure 6

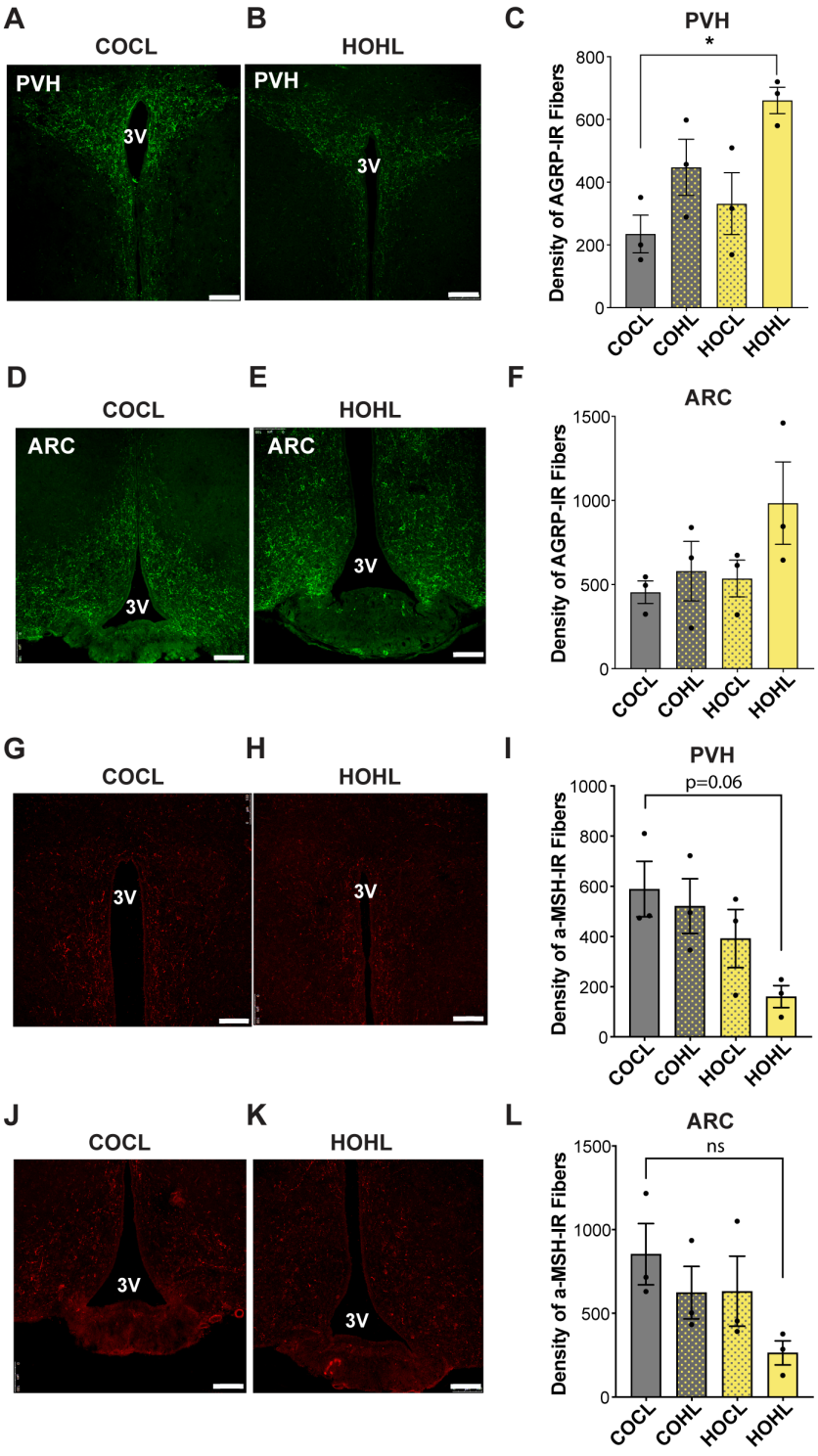
A
COCL
PVH
3V
B
HOHL
PVH
3V
C
PVH
*
Density of AGRP-IR Fibers
800
600
400
200
0
COCL
COHL
HOCL
HOHL
D
COCL
ARC
3V
E
HOHL
ARC
3V
F
ARC
Density of AGRP-IR Fibers
1500
1000
500
0
COCL
COHL
HOCL
HOHL
G
COCL
3V
H
HOHL
3V
I
PVH
p=0.06
Density of a-MSH-IR Fibers
1000
800
600
400
200
0
COCL
COHL
HOCL
HOHL
J
COCL
3V
K
HOHL
3V
L
ARC
ns
Density of a-MSH-IR Fibers
1500
1000
500
0
COCL
COHL
HOCL
HOHL

Figure 7

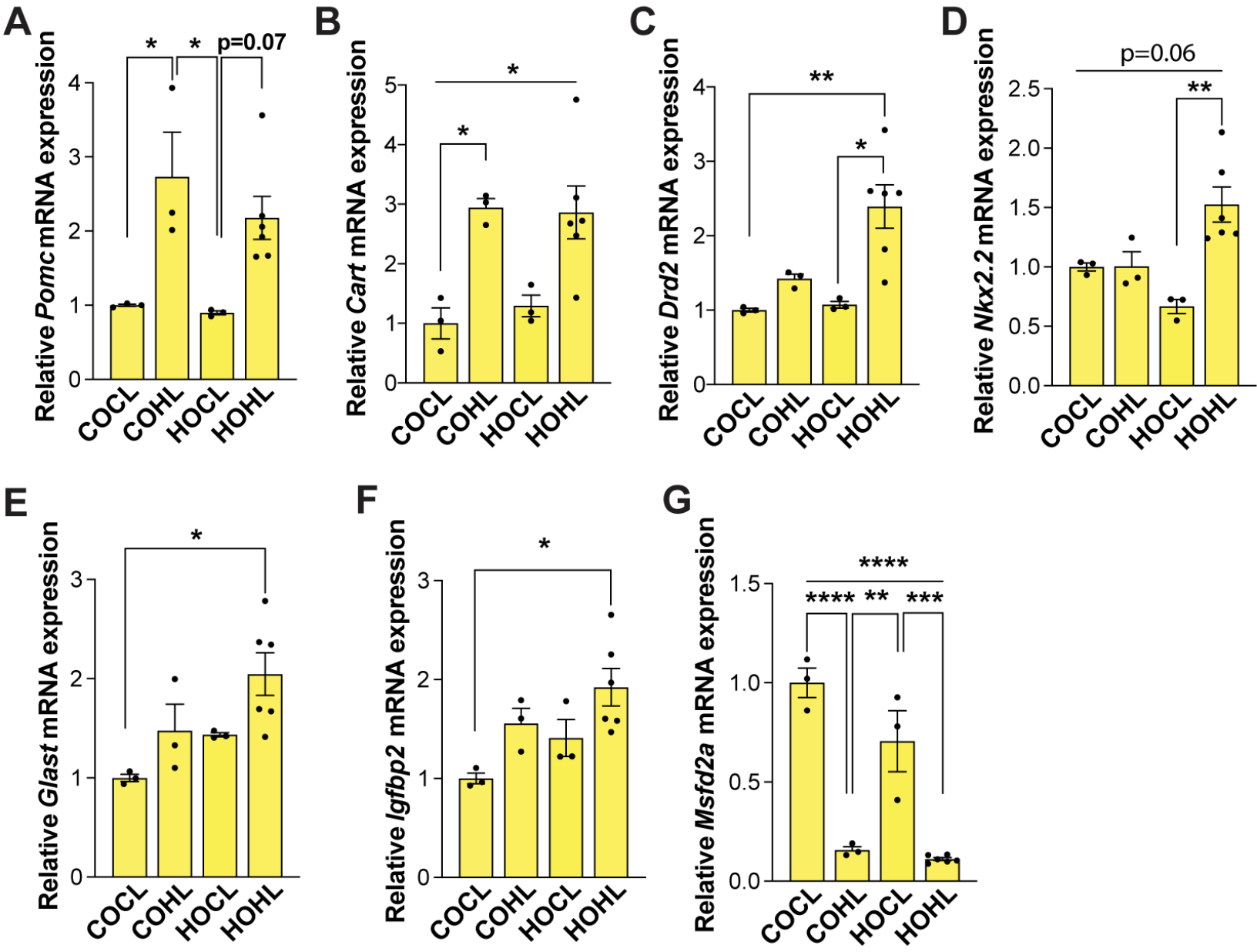
A
Relative Pomc mRNA expression
* * p=0.07
COCL COHL HOCL HOHL
B
Relative Cart mRNA expression
* *
C
Relative Drd2 mRNA expression
** *
D
Relative Nkx2.2 mRNA expression
p=0.06 **
E
Relative Glast mRNA expression
*
F
Relative Igfbp2 mRNA expression
*
G
Relative Msfd2a mRNA expression
**** **** ** ***

Figure 8

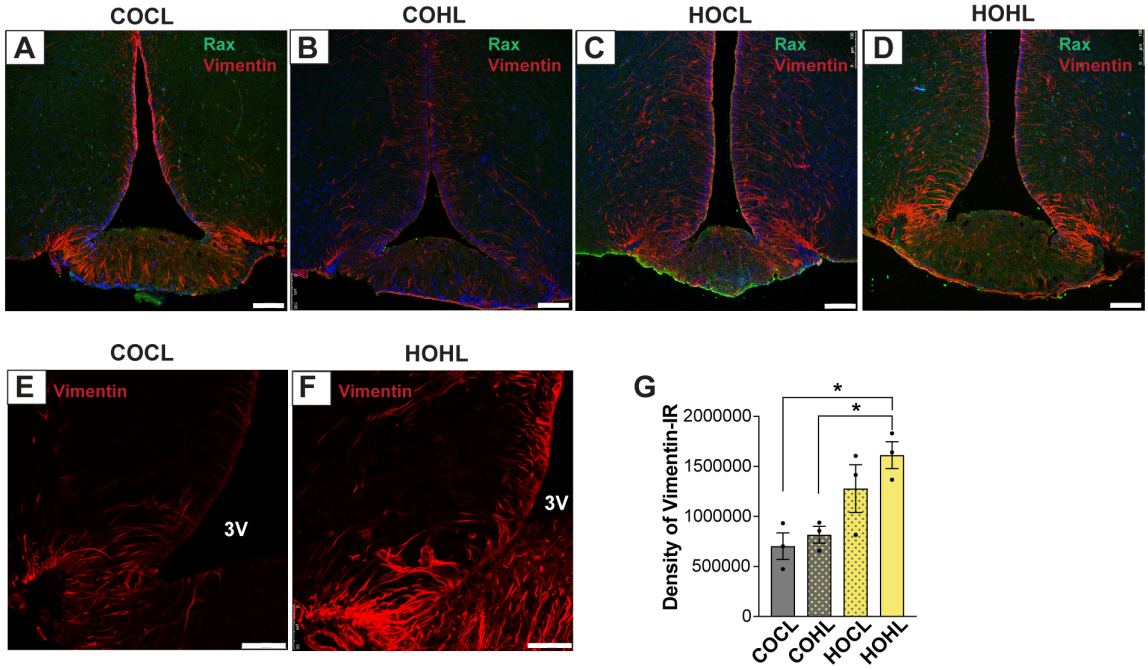
COCL
COHL
HOCL
HOHL
A
B
C
D
Rax
Vimentin
E
F
Vimentin
3V
G
Density of Vimentin-IR
2000000
1500000
1000000
500000
0
*
*
COCL
COHL
HOCL
HOHL

Applied Biosystems probe included primers	Assay	Ref Seq	Exon Location
Agrp	Mm00475829_g1	NM_001271806.1	3-4
Bmp7	Mm00432102_m1	NM_007557.3	3-4
Cartpt	Mm04210469_m1	NM_001081493.2	2-3
Cav	Mm00483057_m1	NM_001243064.1	1-2
Cd11b	Mm00434455_m1	NM_001082960.1	3-4
Crh	Mm01293920_s1	NM_205769.2	2-2
Cx3cl1	Mm00436454_m1	NM_009142.3	1-2
Drd2	Mm00438545_m1	NM_010077.2	7-8
Fgf10	Mm00433275_m1	NM_008002.4	1-2
Gapdh	Mm99999915_g1	NM_008084.2	2-3
Gfap	Mm01253033_m1	NM_001131020.1	6-7
Glast	Mm00600697_m1	NM_148938.3	3-4
Glut	Mm00441480_m1	NM_011400.3	8-9
Hcrt	Mm01964031_s1	NM_010410.2	2-2
Igfbp2	Mm00805581_m1	NM_183029.2	6-7
Il1β	Mm00434228_m1	NM_008361.3	3-4
Il6	Mm00446190_m1	NM_031168.1	2-3
Il10	Mm01288386_m1	NM_010548.2	4-5
Nkx2.2	Mm00839794_m1	NM_001077632.1	1-2
Npy	Mm00445771_m1	NM_023456.2	2-3
Pomc	Mm00435874_m1	NM_001278581.1	3-4
Sox2	Mm03053810_s1	NM_011443.3	1-1
Th	Mm00447557_m1	NM_009377.1	12-13
Tgfb	Mm01178820_m1	NM_011577.1	5-6
Tnf	Mm00443258_m1	NM_001278601.1	1-2
Trh	Mm01182425_g1	NM_009426.3	2-3
Vegf	Mm00437306_m1	NM_001025250.3	3-4
Integrated DNA Technologies probe not included primers	**Assay**	**Ref Seq**	**Exon Location**
Ang	Mm.PT.58.41283141	NM_001161731	1-3
Angpt1	Mm.PT.58.43888746	NM_009640	8-9
Ctnnb1	Mm.PT.58.12501105	NM_007614	10-11
Edn1	Mm.PT.58.42871461	NM_010104	1-2
Ednra	Mm.PT.58.33133227	NM_010332	5-6
Gapdh	Mm.PT.39a.1	NM_008084	2-3
Igf1	Mm.PT.58.5811533	NM_184052	4-5b

Msfd2a	Mm.PT.58.32675283	NM_029662	13-14
Nestin	Mm.PT.58.5953887	NM_016701	2-3
Sema3a	Mm.PT.58.11314988	NM_001243073	17-18
Shh	Mm.PT.58.14105875	NM_009170	2-3
Wnt5a	Mm.PT.58.16402801	NM_009524	5-6
Wnt7a	Mm.PT.58.10737548	NM_009528	5-6

Gene	Fold Regulation	p-Value
Actn3	2.46	0.000000
Actn4	2.01	0.000000
Zak	2.35	0.000000
Cask	2.37	0.000000
Cd99	2.14	0.000000
Cldn1	3.85	0.000000
Cldn10	2.39	0.000000
Cldn11	2.35	0.000000
Cldn14	2.69	0.000000
Cldn15	2.85	0.000000
Cldn18	2.51	0.000000
Cldn4	6.19	0.000000
Cldn5	2.33	0.000000
Cldn8	3.59	0.000000
Cldn7	2.34	0.000000
Ybx3	2.33	0.000000
Csnk2a1	2.48	0.000000
Csnk2a2	2.31	0.000000
Csnk2b	2.72	0.000000
Ctnna2	2.63	0.000000
Ctnna3	2.11	0.000000
Ctnna4	3.1	0.000000
Cttn	2.36	0.000000
Epb4.1	2.48	0.000000
Esam	2.93	0.000000
Gnai1	2.12	0.000000
Icam1	2.25	0.000000
Ilk	2.2	0.000000
Magi3	2.47	0.000000
Mllt4	2.16	0.000000
Mpp6	2.08	0.000000
Pard3	2.41	0.000000
Pard6a	3.36	0.000000
Pecam1	2.08	0.000000
Prkcz	2.35	0.000000
Pten	2.39	0.000000
Smurf1	3.26	0.000000
Sptb	2.16	0.000000
Tiam1	2.1	0.000000
Tjp1	2.14	0.000000
Tjp2	2.04	0.000000

Vapa	**2.36**	0.000000
Gusb	**2.09**	0.000000
MGDC	**3.14**	0.000000

Gene	Fold Regulation	p-Value
Actn3	-7.7	0.000000
Cldn16	-2.01	0.000000
Cldn6	2.96	0.000000